Sensitivity to Neutralizing Antibodies and Resistance to Type I Interferons in SARS-CoV-2 R.1 Lineage Variants, Canada

Rajesh Abraham Jacob, Ali Zhang,[1] Hannah O. Ajoge,[1] Michael R. D'Agostino,[1] Kuganya Nirmalarajah, Altynay Shigayeva, Wael L. Demian, Sheridan J.C. Baker, Hooman Derakhshani, Laura Rossi, Jalees A. Nasir, Emily M. Panousis, Ahmed N. Draia, Christie Vermeiren, Jodi Gilchrist, Nicole Smieja, David Bulir, Marek Smieja, Michael G. Surette, Andrew G. McArthur, Allison J. McGeer, Samira Mubareka, Arinjay Banerjee, Matthew S. Miller, Karen Mossman

Isolating and characterizing emerging SARS-CoV-2 variants is key to understanding virus pathogenesis. In this study, we isolated samples of the SARS-CoV-2 R.1 lineage, categorized as a variant under monitoring by the World Health Organization, and evaluated their sensitivity to neutralizing antibodies and type I interferons. We used convalescent serum samples from persons in Canada infected either with ancestral virus (wave 1) or the B.1.1.7 (Alpha) variant of concern (wave 3) for testing neutralization sensitivity. The R.1 isolates were potently neutralized by both the wave 1 and wave 3 convalescent serum samples, unlike the B.1.351 (Beta) variant of concern. Of note, the R.1 variant was significantly more resistant to type I interferons (IFN-α/β) than was the ancestral isolate. Our study demonstrates that the R.1 variant retained sensitivity to neutralizing antibodies but evolved resistance to type I interferons. This critical driving force will influence the trajectory of the pandemic.

SARS-CoV-2 continues to evolve and generate new variants. Since the beginning of the COVID-19 pandemic, Canada has encountered 8 waves of infections. Although the first 2 waves were dominated by ancestral viruses, each subsequent wave had a surge in escape variants (*1*,*2*). Mutations in the SARS-CoV-2 genome and within the spike glycoprotein alter the transmission dynamics, severity of disease, and sensitivity to neutralizing antibodies for each new variant (*3*). Thus, continuously isolating and characterizing emerging SARS-CoV-2 variants is critical for developing updated vaccines and drug regimens.

We isolated SARS-CoV-2 R.1 lineage variants from an outbreak in persons facing housing insecurity in Hamilton, Ontario, Canada. In Canada, the circulation of R.1 lineage variants corresponded with the third wave of the pandemic and was preceded by previously circulating variants of concern (VoC), B.1.1.7 (Alpha) and B.1.351 (Beta). Globally, the R.1 lineage began to increase in frequency in December 2020, peaked in April 2021, became rare by June 2021, and was last reported in December 2021 (*4*). In April 2021, the World Health Organization positioned R.1 lineage variants under the variant under monitoring (VuM) category to prioritize monitoring the variants because of distinct mutations in their genome. Most infections with R.1 variants have been reported in Japan and the United States (*5*,*6*). In Canada, 66 R.1 lineage sequences were recorded, according to GISAID (https://www.gisaid.org), during December 2020–

Author affiliations: McMaster University, Hamilton, Ontario, Canada (R.A. Jacob, A. Zhang, H.O. Ajoge, M.R. D'Agostino, W.L. Demian, S.J.C. Baker, L. Rossi, J.A. Nasir, E.M. Panousis, A.N. Draia, D. Bulir, M. Smieja, M.G. Surette, A.G. McArthur, M.S. Miller, K. Mossman); Sunnybrook Research Institute, Toronto, Ontario, Canada (K. Nirmalarajah, S. Mubareka); University of Toronto, Toronto (A. Shigayeva, C. Vermeiren, A.J. McGeer, S. Mubareka, A. Banerjee); University of Manitoba, Winnipeg, Manitoba, Canada (H. Derakhshani); Research Institute of St. Joe's Hamilton, Hamilton (J. Gilchrist, N. Smieja, D. Bulir); Vaccine and Infectious Disease Organization, Saskatoon, Saskatchewan, Canada (A. Banerjee); University of Saskatchewan, Saskatoon (A. Banerjee); University of Waterloo, Waterloo, Ontario, Canada (A. Banerjee); University of British Columbia, Vancouver, British Columbia, Canada (A. Banerjee)

DOI: https://doi.org/10.3201/eid2907.230198

[1]These authors contributed equally to this article.

November 2021 (*4*). Of those, 63 originated from Ontario, 1 each originated from Quebec and British Columbia, and 1 originated from an unknown province or territory. However, data on the immune-evasive properties of this lineage variant are limited.

The type I interferon (IFN) response constitutes the first line of defense against many viruses (*5*,*6*), triggering activation of several IFN-stimulated genes (ISGs) and establishing an antiviral state (*5*). SARS-CoV-2 proteins are involved in IFN evasion either by directly suppressing production or by acting downstream of the host response machinery (*6*,*7*). A recent study compared multiple type I IFNs against diverse SARS-CoV-2 VoC, demonstrating increased IFN resistance (*8*). Furthermore, SARS-CoV-2–infected persons with genetic defects in IFN signaling are at higher risk for severe COVID-19 (*9*). Taken together, characterizing IFN-resistant SARS-CoV-2 variants is critical, given their potential to enhance transmission kinetics and result in viral evolution. Therefore, we evaluated the sensitivity of SARS-CoV-2 R.1 lineage isolates from patients in Canada to neutralizing antibodies and type I interferons.

Methods

Cells and Viruses

Vero E6 cells and Calu-3 cells were cultured in complete media (Appendix, https://wwwnc.cdc.gov/EID/article/29/7/23-0198-App1.pdf). We isolated and purified study isolate SB3 as described previously (*10*) and isolated the R.1 lineage variant from patient nasopharyngeal swab samples (Appendix). We obtained the B.1.351 (Beta) VoC isolate from BEI Resources (https://www.beiresources.org).

Human Donors

We obtained informed consent for the collection of convalescent serum samples from 39 patients with quantitative reverse transcription PCR (qRT-PCR)–confirmed SARS-CoV-2 infection (Appendix). This study was approved by the institutional review board for Sunnybrook Research Institute (approval no. 2218) and Sinai Health System (approval nos. 02-0118-U and 05-0016-C).

SARS-CoV-2 Sequencing and Phylogenetic Tree

We performed sequencing of SARS-CoV-2 genomes from RNA extracts and subsequent bioinformatics analysis following the steps detailed in Kotwa et al. (*11*) (Appendix). We constructed a maximum-likelihood phylogenetic tree using a dataset of study sequences (R.1 645, R.1 646, and SB3), Los Alamos National Laboratories full-length variant reference alignment from GISAID (*12*), and randomly sampled Alpha, Beta, and Gamma variant sequences (Appendix).

Detection of SARS-CoV-2–Specific Binding Antibodies and Neutralization Assay

We determined the IgG targeting the receptor-binding domain (RBD) and spike S1 region by using ELISA (BioLegend, https://www.biolegend.com) (Appendix). We performed neutralization assays by incubating serially diluted serum samples (heat inactivated) with SARS-CoV-2 (15,000, 1,500, or 150 PFU/well) at 37°C for 1 h before adding them to preplated Vero E6 cells. Five days after infection, we quantified luminescence with CellTiter-Glo 2.0 Reagent (Promega, https://www.promega.com) by using a BioTek Synergy H1 microplate reader (Appendix).

Molecular Detection of SARS-CoV-2 $N_{501}Y$ Mutation

Diagnostic nasopharyngeal or midturbinate swab specimens were collected from patients for SARS-CoV-2 testing and $N_{501}Y$ screening at Shared Hospital Laboratory (Toronto, Canada). We performed RNA extraction and qRT-PCR to detect SARS-CoV-2 as previously described (*13*) (Appendix).

Interferon Treatment and Quantitative PCR

Calu-3 cells were either mock-infected or SARS-CoV-2–infected (1 h exposure, 50,000 PFU/well), washed twice with sterile 1× phosphate-buffered serum, and treated with 1 ng/mL or 10 ng/mL of recombinant IFN-α (Sigma-Aldrich, https://www.sigmaaldrich.com) or IFNβ (PeproTech, https://www.peprotech.com). We quantified SARS-CoV-2 RNA and ISGs 72 h postinfection by using qRT-PCR (Appendix).

Viability Assay, Microscopy, and Statistical Analysis

We assessed cell viability of SARS-CoV-2–infected Calu-3 cells by using CellTiter-Glo 2.0 Reagent (Promega) (Appendix) and imaged SARS-CoV-2–infected Calu-3 cells for cytopathic elects using an EVOS M5000 microscope (ThermoFisher Scientific, https://www.thermofisher.com) with the 10× objective. We performed all statistical analyses by using GraphPad Prism (https://www.graphpad.com) (Appendix).

Results

R.1 Lineage Variant Virus Isolation and Lineage Determination

We isolated 2 SARS-CoV-2 isolates belonging to the R.1 lineage (R.1 645, R.1 646) from 2 patients from Hamilton, Ontario, Canada, in March 2021, corresponding to the third wave of the COVID-19

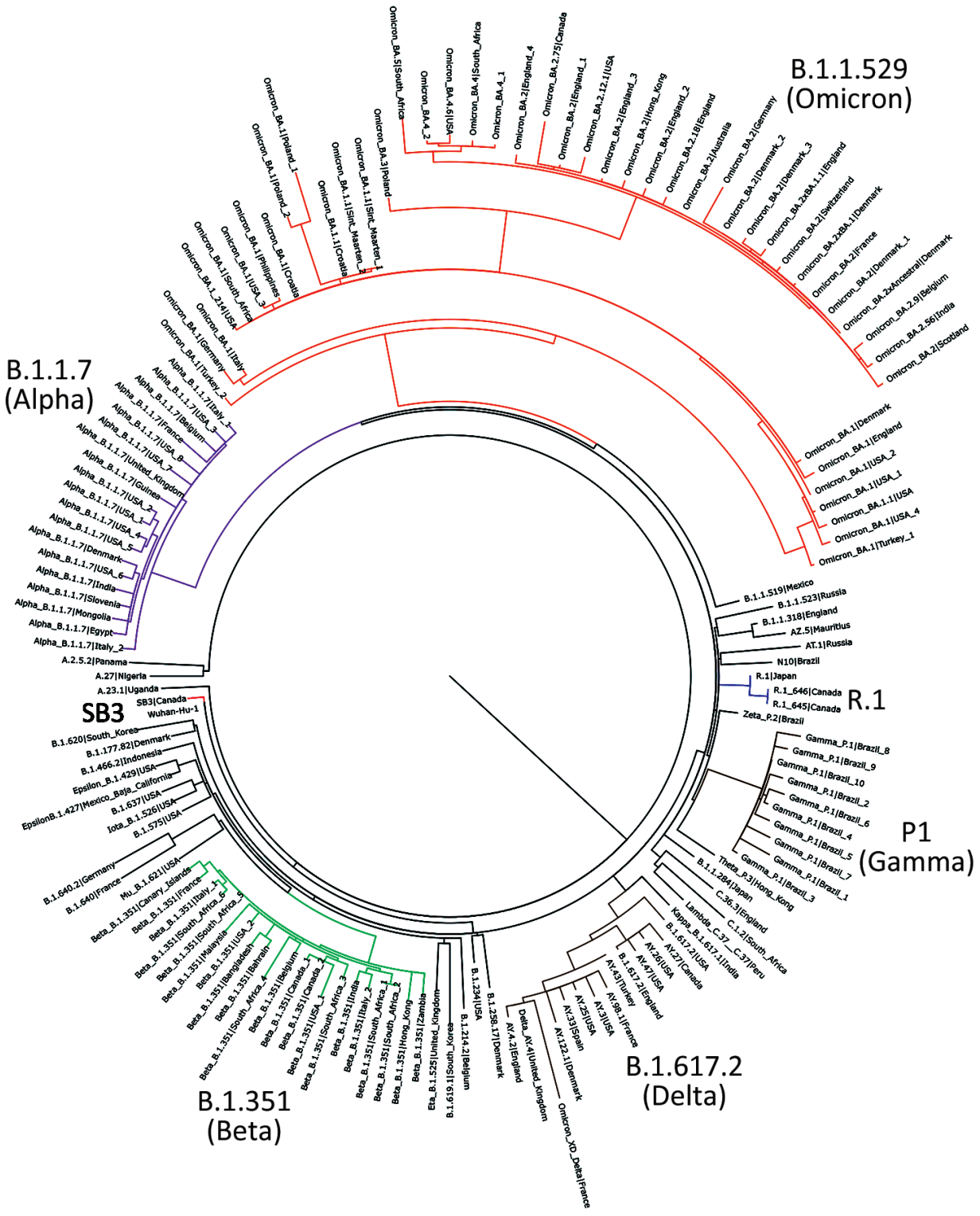

Figure 1. Phylogenetic confirmation that SARS-CoV-2 isolates belong to R.1 lineage in study of sensitivity to neutralizing antibodies and resistance to type I interferons in SARS-CoV-2 R.1 lineage variants, Canada. Tree constructed by using maximum-likelihood estimations by executing 1,000 rapid bootstrap inferences and a thorough search with the general time reversible model of nucleotide substitution. Blue indicates R1 isolates (R.1 645, R.1 646) and red SB3 isolate. Variants are highlighted in magenta (Alpha), green (Beta), brown (Delta), mocha (Gamma), and orange (Omicron). The tree was visualized using FigTree version 1.4.2 (http://tree.bio.ed.ac.uk/software/figtree).

pandemic in Canada. The 2 R.1 isolates were purified from nasopharyngeal samples from SARS-CoV-2–specific qRT-PCR–positive persons by using Vero clone E6 cells as described previously (*10*). We determined the viral whole-genome sequences and deposited them into GISAID (accession nos. EPI_ISL_16641180 and EPI_ISL_16641181). We performed phylogenetic analysis to confirm clustering with the R.1 lineage. The R.1 isolates clustered on their own distinctly from B.1.1.7 (Alpha), B.1.351 (Beta), B.1.617.2 (Delta), P.1 (Gamma), and B.1.1.529 (Omicron) variants (Figure 1). Sequencing of both R.1 isolates revealed multiple mutations in spike ($W_{152}L$, $S_{255}F$, $E_{484}K$, $D_{614}G$, $G_{769}V$), nonstructural protein (NSP) 2 ($P_{129}L$, $A_{247}V$), NSP3 ($S_{1656}A$), NSP12 ($P_{323}L$), NSP13 ($G_{439}R$, $P_{323}L$), NSP14 ($P_{412}H$), ORF3a ($R_{134}H$), membrane ($F_{28}L$), and the nucleocapsid ($S_{187}L$, $R_{203}K$, $G_{204}R$, $Q_{418}H$) regions critical to immune evasion (*14*).

Wave 1 and Wave 3 Serum Samples

We next characterized the R.1 isolates to identify potential effects on the epidemiology of COVID-19. We assessed the susceptibility of R.1 isolates to neutralizing antibodies after SARS-CoV-2 infection in a cohort of patients who had recovered from laboratory-confirmed COVID-19 by collecting convalescent serum samples from 39 unvaccinated donors during the first (n = 26) and third (n = 13) waves of the pandemic in Canada. The cohort consisted of 20 men and 19 women with a median age of 58. Wave 1 consisted of 13 men and 13 women with a median age of 63. Wave 3 consisted of 7 men and 6 women with a median age of 53. Samples were collected a median of 42 days after the first qRT-PCR–positive test. Most patients were symptomatic and more than one third were hospitalized; a subset of hospitalized patients was admitted to the intensive care unit (Table 1).

Wave 1 (March–June 2020) was dominated by infection with the SARS-CoV-2 ancestral strain, whereas wave 3 (March–May 2021) was dominated by infection with the B.1.1.7 (Alpha) VoC (*2*,*15*). A key amino acid change in the RBD of the B.1.1.7 (Alpha) VoC was the $N_{501}Y$ substitution (*16*). We initially used qRT-PCR screening to confirm the presence of the $N_{501}Y$ mutation in the 13 clinical samples from wave 3 patients. The $N_{501}Y$ substitution enhances the affinity of RBD to the angiotensin-converting enzyme 2 receptor (*17*,*18*) and is present in the B.1.1.7 (Alpha), B.1.351 (Beta), P.1 (Gamma), and B.1.1.529 (Omicron) lineages but not in the R.1 lineage variants (*19*–*21*). Whole-genome sequencing confirmed that the wave 3 variant with the $N_{501}Y$ substitution belonged to the B.1.1.7 (Alpha) VoC. For this investigation, we elicited antibodies from wave 1 serum samples (n = 26) by infection with viruses harboring the ancestral SARS-CoV-2 spike, whereas we elicited antibodies from wave 3 serum samples (n = 13) by viruses harboring the B.1.1.7 (Alpha) VoC spike.

Determination of SARS-CoV-2 Spike- and RBD-Binding Antibodies

Initially, we determined the binding ability of waves 1 and 3 serum samples to SARS-CoV-2 ancestral antigens using ELISA. We detected binding antibodies targeting the SARS-CoV-2 spike (S1 subunit) and RBD. Plates coated with either the ancestral S1 or the ancestral RBD were used to detect binding IgG. Antibodies from waves 1 and 3 serum samples bound the ancestral S1 and ancestral RBD (Figure 2, panels A, B). IgG levels from wave 1 serum samples were comparable

Table 1. Clinical summary of patients from study of sensitivity to neutralizing antibodies and resistance to type I interferons in SARS-CoV-2 R.1 lineage variants, Canada*

Characteristic	Value
Total no. samples	39
No. samples, wave 1	26
No. samples, wave 3	13
Median age, total (IQR)	58 (46–68)
Median age, wave 1 (IQR)	63 (55–71)
Median age, wave 3 (IQR)	53 (33–56)
Sex, total	
M	20
F	19
Sex, wave 1	
M	13
F	13
Sex, wave 3	
M	7
F	6
Median no. days to sampling from first COVID-19 positive test (IQR)	42 (25–71)
Hospital admission	14 (36)
Median days from symptom onset to admission (IQR)	6 (2–10)
Symptoms	
Asymptomatic	1 (2)
Fever	17 (43)
Cough	19 (54)
Shortness of breath	8 (20)
Comorbidities	
Diabetes	9 (23)
Cardiac illnesses	4 (10)
Vascular illnesses	13 (33)
Pulmonary illnesses	3 (8)
Renal illnesses	2 (5)
Neuromuscular illnesses	0 (0)
Liver illnesses	0 (0)
Gastrointestinal illnesses	0 (0)
Cancer conditions	3 (7)
Rheumatologic illnesses	1 (2)
Mental health diagnosis	3 (7)
Immunocompromised	0 (0)
ICU admission	4 (10)
Intubation	2 (5)

*Values are no. (%) except as indicated. ICU, intensive care unit; IQR, interquartile range.

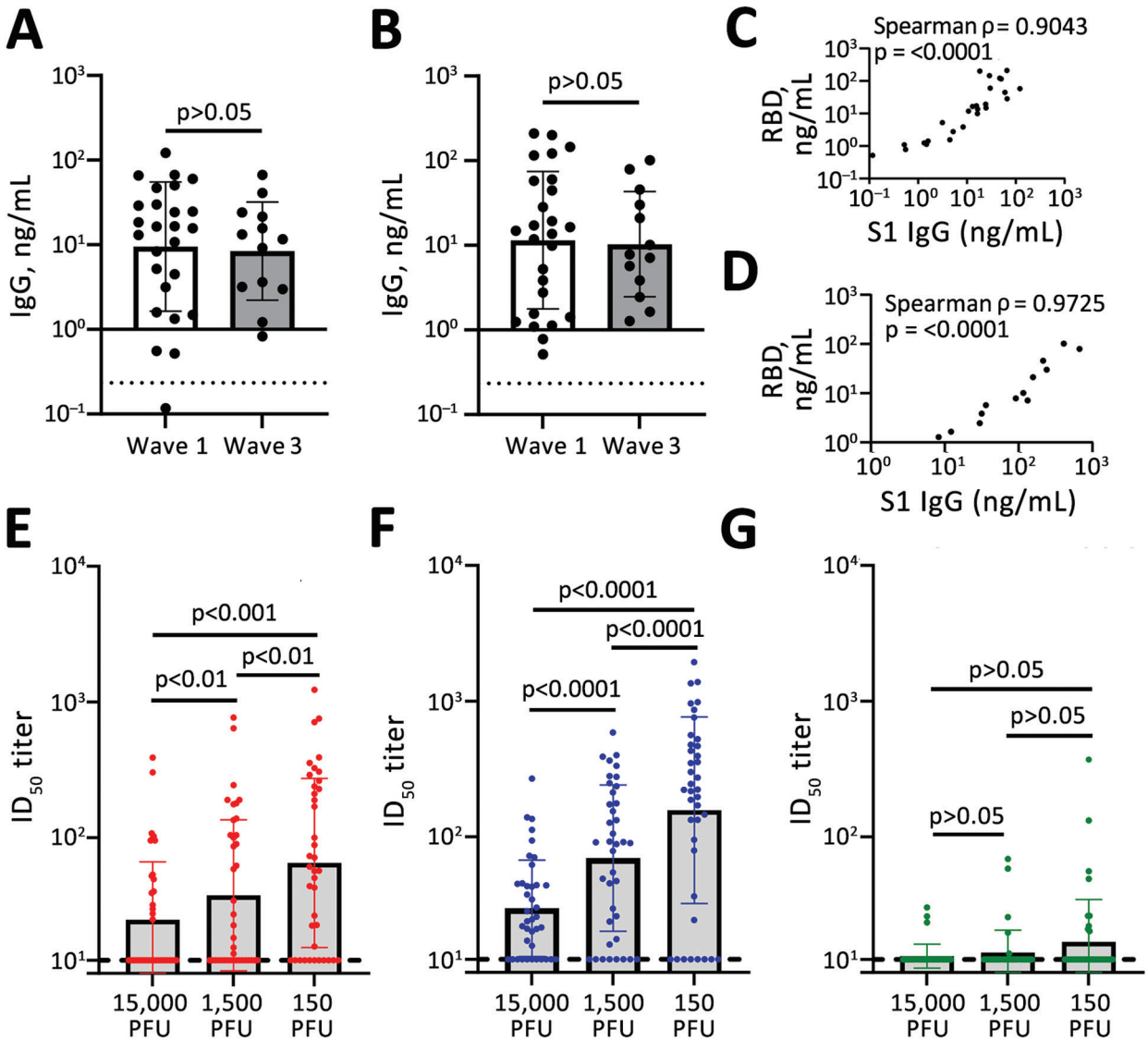

Figure 2. Antibody detection in study of sensitivity to neutralizing antibodies and resistance to type I interferons in SARS-CoV-2 R.1 lineage variants, Canada. A, B) S1 (A) and RBD (b) binding IgG determined by using a sandwich ELISA format. Dashed line indicates the limit of detection. C, D) Correlation between S1 and RBD binding IgG for wave 1 (C) and wave 3 (D). E–G) ID50 titers for SB3 (E), R.1 645 (F), and B.1.351 (Beta) VoC (E). Error bars in panels A, B and E–G indicate SD. Statistical significance was calculated by using an unpaired t test for panels A and B and by using 1-way analysis of variance with Tukey multiple comparisons test for panels E–G. ID_{50}, 50% inhibitory dilution; PFU, plaque-forming units; RBD, receptor-binding domain; S1, spike.

to wave 3 serum samples for both the S1 (geometric mean 9.51 vs. 8.42 ng/mL) and the RBD (geometric mean 11.47 vs. 10.30 ng/mL) (Figure 2, panels A and B). This observation indicates that binding antibodies generated by the B.1.1.7 (Alpha) VoC in wave 3 were cross-reactive with the ancestral S1 and ancestral RBD.

Next, we investigated the correlation between S1-targeting IgG and the RBD-targeting IgG. The S1 and the RBD targeting IgG correlated well; for both wave 1 (Spearman ρ = 0.9043; p<0.0001) and wave 3 serum samples (Spearman ρ = 0.9725; p<0.0001) (Figure 2, panels C. D). This correlation indicates that for both wave 1 and wave 3 serum samples, the ancestral S1 and RBD antigens were equally available for binding.

Neutralization of SB3, R.1 645, and B.1.351 (Beta) VoC

Next, we assessed the antibody function by using a neutralization assay for the entire cohort. We compared the neutralization sensitivity of the R.1 isolates with SB3 and B.1.351 (Beta) VoC. Live SARS-CoV-2

isolates were used for the neutralization assay. SB3 is an ancestral isolate purified from a SARS-CoV-2–infected patient in early 2020 from Toronto, Canada (*10*). B.1.351 is a highly neutralization-resistant isolate that was first detected in late 2020 from Eastern Cape, South Africa (*22*). B.1.351 has extensive mutations in the spike region ($L_{18}F$, $D_{80}A$, $D_{215}G$, $\Delta_{242-244}$, $K_{417}N$, $E_{484}K$, $N_{501}Y$, $D_{614}G$, and $A_{701}V$), conferring resistance to antibodies from both convalescent and vaccinated persons (*22*–*26*).

To establish a robust readout for neutralization, we tested 3 different plaque-forming unit (PFU) levels (15,000, 1,500, and 150) per well for all 3 isolates (SB3, R.1 645, and B.1.351 [Beta] VoC). We generated neutralization profiles for SB3 (Appendix Figure 1, panels A–C), R.1 645 (Appendix Figure 1, panels D–F), and B.1.351 (Appendix Figure 1, panels G–I) and derived 50% inhibitory dilution (ID_{50}) values. For SB3, we observed a significant difference in ID_{50} between the 3 different PFUs tested; 150 PFU/well was the most neutralization sensitive and 15,000 PFU/well the most resistant (Figure 2, panel E). The geometric means of ID_{50} titers were 24.9 for 15,000 PFU/well, 37.7 for 1,500 PFU/well, and 65.2 for the 150 PFU/well (Figure 2, panel E). As for SB3, the geometric mean of R.1 645 ID_{50} titers increased from 29.7 for 15,000 PFU/well to 69.6 for 1,500 PFU/well and 156.9 for 150 PFU/well (Figure 2, panel F). However, for B.1.351, we noticed no significant difference among the 3 PFUs tested. The geometric mean of ID_{50} titers remained very low: 13.2 for 15,000 PFU/well, 14.0 for 1,500 PFU/well, and 16.9 for 150 PFU/well (Figure 2, panel G), corroborating previous data that B.1.351 is highly resistant to neutralization (*23*–*25*). This neutralization profile shows that the serum samples have diverse neutralizing abilities; titers significantly increased as the number of viral particles decreased for SB3 and R.1 645 but not for the highly resistant B.1.351.

Sensitivity of R.1 645 and R.1 646 to Neutralizing Antibodies

Next, we determined whether the 2 R.1 isolates (R.1 645, R.1 646) had similar sensitivity to neutralizing antibodies by screening a subset of the serum samples (n = 19 from wave 1 and 3) on R.1 646 (Appendix Figure 2, panels A–C). The Spearman rank correlation coefficient (ρ) values remained high for 15,000 (Spearman $\rho = 0.8333$; $p<0.0001$), 1,500 (Spearman $\rho = 0.9262$; $p<0.0001$), and 150 (Spearman $\rho = 0.8677$; $p<0.0001$) PFU/well (Appendix Figure 2, panels D–F), indicating that the R.1 isolates were similarly neutralized by the serum samples.

Binding IgG as a Prediction of SARS-CoV-2 Neutralization

We next assessed whether binding antibodies are predictive of SARS-CoV-2 neutralization. We used a linear regression model to predict whether the RBD and spike (S1) targeting IgG could neutralize SB3, R.1 645, and B.1.351 (Beta) VoC, using only the 150 PFU/well condition because it had the highest neutralization titers. RBD-binding IgG were a weak predictor of SB3 ($R^2 = 0.3819$; $p<0.0001$) and R.1 645 ($R^2 = 0.2225$; $p = 0.0024$) neutralization, but we noted no significance for B.1.351 (Beta) VoC ($R^2 = 0.05892$; $p>0.05$) (Appendix Figure 3, panel A). In contrast to RBD, the neutralization prediction was moderately improved for S1-binding IgG for SB3 ($R^2 = 0.5148$; $p<0.0001$) and R.1 645 ($R^2 = 0.6025$; $p<0.0001$) but weak for B.1.351 ($R^2 = 0.1308$; $p<0.0001$) (Appendix Figure 3, panel B). Those data suggest that S1-targeting antibodies outside the RBD are markedly involved in neutralization.

Neutralization of R.1 Isolate by Wave 1 Serum Samples

Next, we determined whether the R.1 isolate (R.1645) that emerged during wave 3 was sensitive to neutralizing antibodies elicited by the ancestral virus from wave 1. To test this possibility, we compared the neutralization susceptibility of R.1 645 with SB3 and B.1.351 (Beta) VoC. We observed no significant difference in the ID_{50} titers between SB3 and R.1 645 at higher PFUs (15,000 and 1,500) (Figure 3, panels A, B). However, R.1 645 was significantly more sensitive than SB3 at 150 PFU/well; we noted a 1.6-fold increase in the geometric mean of the ID_{50} titers (Figure 3, panel C). Furthermore, R.1 645 was significantly more sensitive than B.1.351 at all 3 PFUs tested (Figure 3, panels A–C). A 2.2-fold, 4.5-fold, and 8.2-fold increase in the geometric mean of ID_{50} titers was noted for R.1 645 in comparison to B.1.351 (Figure 3, panels A–C). SB3 also remained significantly more sensitive than B.1.351 at lower PFUs (3.3-fold increase in geometric mean of ID_{50} titers at 1,500 PFU/well and 5-fold increase at 150 PFU/well) (Figure 3, panels B, C). This observation indicates that the R.1 isolate, despite having spike mutations, remains sensitive to antibodies from wave 1 serum samples (Table 2).

Neutralization of R.1 Isolate by Wave 3 Serum Samples

Subsequently, we analyzed whether the antibodies elicited by the B.1.1.7 (Alpha) VoC during wave 3 of the pandemic can neutralize the R.1 isolate. A significant increase in the ID_{50} titers was notable between SB3 and R.1 645 at all the PFUs tested (Figure 3, panels D–F). We noted 1.6-fold, 3.5-fold, and 5.1-fold increases in the geometric mean of the ID_{50} titers for R.1 645 in

Table 2. Summary of neutralization of SARS-CoV-2 isolates from study of sensitivity to neutralizing antibodies and resistance to type I interferons in SARS-CoV-2 R.1 lineage variants, Canada

SARS-CoV-2 isolates	Sensitive isolate	Adjusted p value
Wave 1: 15,000 PFU		
SB3 vs. R.1 645	NA	NS
SB3 vs. B.1.351	NA	NS
R.1 645 vs. B.1.351	R.1645	0.0186
Wave 1: 1,500 PFU		
SB3 vs. R.1 645	NA	NS
SB3 vs. B.1.351	SB3	0.0243
R.1 645 vs. B.1.351	R.1 645	0.0011
Wave 1: 150 PFU		
SB3 vs. R.1 645	R.1 645	0.0141
SB3 vs. B.1.351	SB3	0.0066
R.1 645 vs. B.1.351	R.1 645	0.0022
Wave 3: 15,000 PFU		
SB3 vs. R.1 645	R.1 645	0.0391
SB3 vs. B.1.351	NA	NS
R.1 645 vs. B.1.351	R.1 645	0.0385
Wave 3: 1,500 PFU		
SB3 vs. R.1 645	R.1 645	0.0079
SB3 vs. B.1.351	NA	NS
R.1 645 vs. B.1.351	R.1 645	0.0093
Wave 3: 150 PFU		
SB3 vs. R.1 645	R.1 645	0.0038
SB3 vs. B.1.351	NA	NS
R.1 645 vs. B.1.351	R.1 645	0.0053

*NA, not applicable; NS, not significant; PFU, plaque-forming units.

comparison to SB3. This observation indicates that the antibodies triggered by the B.1.1.7 (Alpha) VoC could neutralize R.1 645 better than SB3. Neutralization titers of R.1 645 also remained high compared with B.1.351 (Beta) VoC, indicating that B.1.351 is significantly resistant to wave 3 serum samples (Figure 3, panels D–F). We noted 2.3-fold, 6.1-fold, and 11.9-fold increases in the geometric mean of ID_{50} titers for R.1 645 in comparison to B.1.351 (Figure 3, panels D–F). However, unlike wave 1 serum samples, we noted no significant difference in the ID_{50} titers between SB3 and B.1.351 for wave 3 serum samples (Figure 3, panels D–F). Those data indicate that the antibody repertoire evolved over time resulting in a substantial loss of neutralization breadth to the ancestral isolate. Of note, the antibody repertoire that evolved in response to the B.1.1.7 (Alpha) VoC during wave 3 could still neutralize the R.1 645 isolate (Table 2).

Sensitivity of R.1 Isolates to Type I Interferons

Next, we investigated the sensitivity of R.1 isolates to type I IFNs. We infected Calu-3 cells with SB3 or one of the 2 R.1 isolates. One hour after absorption, we treated cells with IFN-α or IFN-β (1 ng/mL or 10 ng/mL) for 72 hours. We monitored SARS-CoV-2 RNA levels by using qRT-PCR after isolating total RNA from infected Calu-3 cells to determine the amounts of virus produced 72 hours after infection. As expected, we observed a drop in virus replication with recombinant IFN-α and IFN-β treatment (at both 1 ng/mL and 10 ng/mL concentration) (Figure 4, panels A, B). The R.1 isolates were significantly more resistant to both IFN-α and IFN-β than were SB3 (Figure 4, panels A, B). We observed no significant difference in SARS-CoV-2 RNA levels in the untreated controls. This finding indicates that R.1 isolate resistance to type I IFNs is not caused by differences in the level of incoming virus or inherent replication capacity.

We have previously shown that SARS-CoV-2 is a poor inducer of type I IFN and ISGs (*27*), and others have shown that SARS-CoV-2 can evade the type I IFN machinery (*28*,*29*). Because our R.1 isolates were significantly more resistant to type I IFNs, we examined differences in the expression of 2 ISGs: interferon-induced protein with tetratricopeptide repeats (IFIT1) and interferon regulatory factor 7 (IRF7). We compared the ability of the R.1 isolates to block IFIT1 and IRF7 production in response to IFN to that of SB3. We noted a dose-responsive increase in the transcript levels of *IFIT1* and *IRF7* for both IFN-α– and IFN-β–treated conditions in mock-infected cells (Figure 4, panels C–F). In the presence of SARS-CoV-2, we noted significant suppression of the IFN-α– and IFN-β–mediated activation of *IFIT1* and *IRF7* (Figure 4, panels C–F).). However, we did not observe a significant difference in *IFIT1* or *IRF7* transcript levels between SB3 and the 2 R.1 isolates. We performed a viability assay to confirm that the difference in ISG signal is not caused by SARS-CoV-2–induced cell death (Appendix Figure 4, panels A, B). The absence of SARS-CoV-2–induced

cytopathic effect corroborates our viability data (Appendix Figure 5, panels A, B) and is consistent with other studies (*30*,*31*). This observation implies that the resistance of the R.1 isolates to type-I IFNs is not inherently dependent on ISG modulation.

Discussion

We demonstrate that R.1 isolates are sensitive to neutralizing antibodies induced after natural SARS-CoV-2 infection (Figure 3). These results are encouraging and add to our understanding of the sensitivity of VuMs to neutralizing antibodies. We further demonstrate that the R.1 lineage isolates, in contrast to the B.1.351 (Beta) VoC, retain neutralization sensitivity to antibodies generated early and later during the pandemic (Figure 3). Using a pseudovirus-based neutralization assay, a recent study demonstrated that mutations in R.1 lineage drive resistance to neutralizing antibodies compared with the wild type (*32*). Although a good correlation was observed between pseudovirus and live virus assay for antibody neutralization (*33*), a live virus assay more accurately represents spike protein density, epitope exposure, and replication kinetics of SARS-CoV-2. We observed a significant evolution in the breadth of neutralization with wave 3 antibodies, which resulted in a higher neutralization of R.1 isolates compared with the

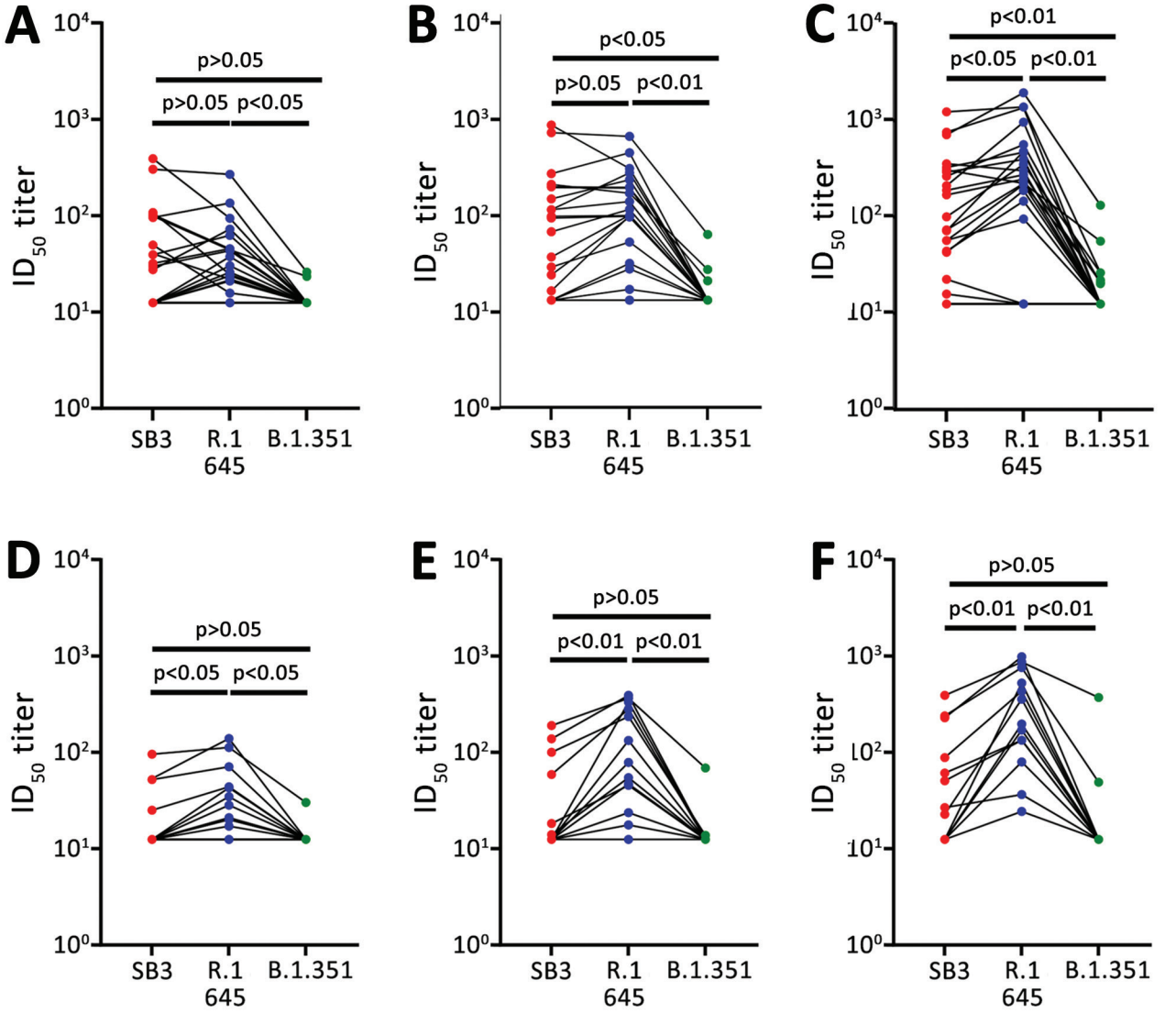

Figure 3. Sensitivity of SARS-CoV-2 lineage variants to neutralizing antibodies, Canada. A–C) Sensitivity of SB3, R.1 645, and B.1.351 (Beta) variants to neutralizing antibodies from patients infected with the ancestral virus (wave 1 samples). D–F) Sensitivity of SB3, R.1 645, and B.1.351 (Beta) VoC to neutralizing antibodies from patients infected with the B.1.1.7 (Alpha) VoC (wave 3 samples). For each isolate, we tested 3 different PFU per well: 15,000 (A, D), 1,500 (B, E), and 150 (C, F). Statistical significance was calculated using 1-way analysis of variance with Tukey multiple comparisons test. ID_{50}, 50% inhibitory dilution; PFU, plaque-forming units.

ancestral isolate (Figure 3, panels D–F). Of the 5 mutations in the spike region of our R.1 isolates, 3 are unique and not found in the B.1.351 (Beta) VoC. These include $W_{152}L$ and $S_{255}F$ substitutions in the N terminal domain of the S1 spike region and the $G_{769}V$ substitution in the S2 domain. A report that investigated key SARS-CoV-2 spike substitutions demonstrated that $W_{152}L$ alone does not confer neutralization resistance (*34*).

We established that the continuum of antibody-mediated neutralization is dependent on the virus

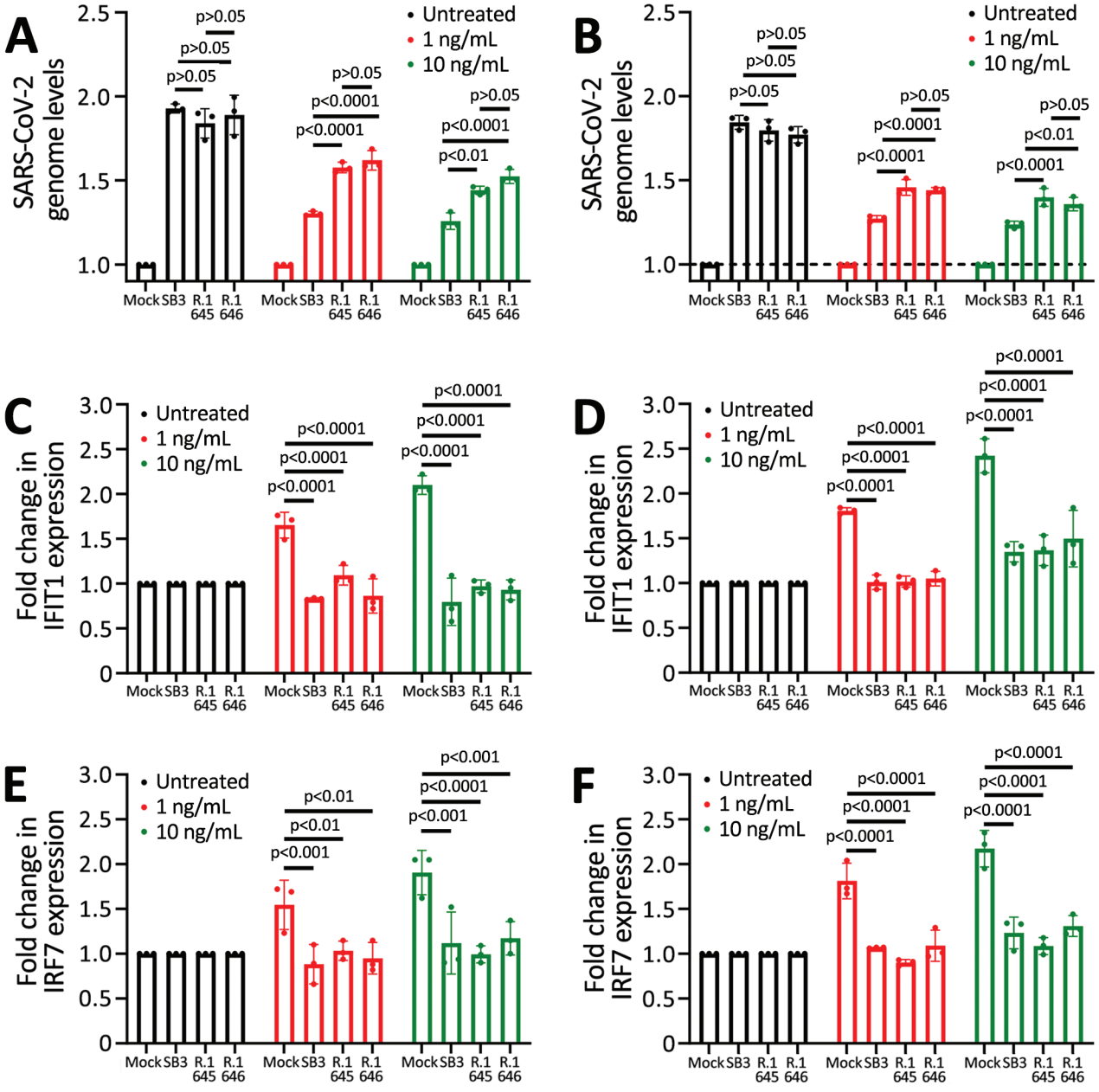

Figure 4. Resistance to type I interferons in SARS-CoV-2 R.1 lineage variants, Canada. A) Sensitivity of SB3, R.1 645, and R.1 646 to IFN-α. B) Sensitivity of SB3, R.1 645, and R.1 646 to IFN-β. C, D) Fold change in *IFIT1* transcript levels in response to IFN-α (C) or IFN-β (D) treatment. E, F) Fold change in *IRF7* transcript levels in response to IFN-α (E) or IFN-β treatment (F). ISG transcript levels were normalized to *GAPDH* transcript levels. For testing, Calu-3 cells were either mock-infected or infected with SARS-CoV-2 (50,000 PFU/well) for 1 hour followed by treatment with recombinant IFN (1 or 10 ng/mL). Total RNA was extracted after 72 hours and SARS-CoV-2 RNA levels were determined using quantitative reverse transcription PCR. 1/ΔCT values are represented after normalizing to mock-infected cells. Statistical significance was calculated using 2-way analysis of variance with Tukey multiple comparisons test. GAPDH, glyceraldehyde 3-phosphate dehydrogenase; IFIT1, interferon-induced protein with tetratricopeptide repeats; IFN, interferon; IRF7, interferon regulatory factor 7; ISG, IFN-stimulated gene.

inoculum (Figure 2, panels E, F) and that different levels of virus inoculum are neutralized differentially for SB3 and R.1 645. A significant drop in the ID_{50} titers was observed as we exponentially increased the number of SARS-CoV-2 particles. Those data imply that the threshold of neutralizing antibody titers necessary for protection is dependent on the exposure dose of virus particles. This finding indicates that a potent humoral response is critical for SARS-CoV-2 protection in vaccinated or naturally infected persons.

Our data show resistance of SARS-CoV-2 variants to type I IFNs, which in turn can influence viral evolution. An increased IFN resistance in SARS-CoV-2 was reported recently (*8*). Our R.1 isolates were significantly resistant to both IFNα and IFNβ treatment within lung epithelial cells (Figure 4, panels A, B). However, whether mutations accumulated in ORF1ab, ORF3, M, and N regions are causing the observed IFN resistance is unclear; this question will be vital in future studies. IFN resistance of R.1 isolates can potentially lead to higher viral loads, thereby accelerating virus shedding and transmission. Although the World Health Organization recategorized R.1 lineage isolates as formerly monitored variants in November 2021, data are limited on the transmission potential and disease severity of the formerly monitored variants. Our finding that R.1 lineage isolates are neutralization sensitive but concurrently IFN resistant indicates that IFN resistance will be a strong driving force in the generation of new variants. Overall, data from this study further advance our knowledge of how virus evolution can influence the trajectory and characteristics of a pandemic.

This work was supported by a COVID-19 response grant to K.M. from the Canadian Institutes of Health Research (CIHR), with sequencing efforts additionally supported by Genome Canada CanCOGeN funding to A.G.M. M.S.M. is supported by a tier 2 Canada Research Chair in Viral Pandemics, a CIHR COVID-19 rapid response grant, a CIHR new investigator award, and an Ontario early researcher award. A.G.M. holds McMaster's inaugural David Braley Chair in Computational Biology, generously supported by the family of the late David Braley. J.A.N. was supported by a Fred and Helen Knight Enrichment Award. Convalescent serum sample collection was supported by a COVID-19 response grant to A.M. and S.M. from CIHR (#439999). Computational support was provided by the McMaster Service Lab and Repository computing cluster, supplemented by hardware donations and loans from Cisco Systems Canada, Hewlett Packard Enterprise, and Pure Storage. Research within A.B.'s laboratory is supported by the Natural Sciences and Engineering Research Council of Canada, CIHR, Saskatchewan Health Research Foundation, and the Coronavirus Variants Rapid Response Network. V.I.D.O. receives operational funding for its CL3 facility (InterVac) from the Canada Foundation for Innovation through the Major Science Initiatives. V.I.D.O. also receives operational funding from the Government of Saskatchewan via Innovation Saskatchewan and the Ministry of Agriculture.

The following reagent was obtained through BEI Resources, NIAID, NIH: SARS-Related Coronavirus 2, Isolate hCoV-19/USA/MD-HP01542/2021 (Lineage B.1.351), in Homo sapiens Lung Adenocarcinoma (Calu-3) Cells, NR-55282, contributed by Andrew S. Pekosz. Homo sapiens lung adenocarcinoma, Calu-3 (HTB-55) and Vero E6 cells (CRL-1586) were obtained from ATCC.

About the Author

Dr. Jacob is a postdoctoral fellow at McMaster University, Hamilton, Canada, and the scientific coordinator for the Canadian Consortium of Academic Biosafety Level 3 Laboratories. His overall research focus is characterizing the molecular and immunological mechanisms underlying virus-host interactions.

References

1. Layton AT, Sadria M. Understanding the dynamics of SARS-CoV-2 variants of concern in Ontario, Canada: a modeling study. Sci Rep. 2022;12:2114. https://doi.org/10.1038/s41598-022-06159-x
2. Tuite AR, Fisman DN, Odutayo A, Bobos P, Allen V, Bogoch II, et al. COVID-19 hospitalizations, ICU admissions and deaths associated with the new variants of concern. Science Briefs of the Ontario COVID-19 Science Advisory Table. 2021 Mar 29 [cited 2023 Feb 1]. https://covid19-sciencetable.ca/sciencebrief/covid-19-hospitalizations-icu-admissions-and-deaths-associated-with-the-new-variants-of-concern
3. Harvey WT, Carabelli AM, Jackson B, Gupta RK, Thomson EC, Harrison EM, et al.; COVID-19 Genomics UK (COG-UK) Consortium. SARS-CoV-2 variants, spike mutations and immune escape. Nat Rev Microbiol. 2021; 19:409–24. https://doi.org/10.1038/s41579-021-00573-0
4. Khare S, Gurry C, Freitas L, Schultz MB, Bach G, Diallo A, et al. GISAID's role in pandemic response. China CDC Wkly.|2021;3:1049–51. https://doi.org/10.46234/ccdcw2021.255
5. Hare D, Mossman KL. Novel paradigms of innate immune sensing of viral infections. Cytokine. 2013;63:219–24. https://doi.org/10.1016/j.cyto.2013.06.001
6. Sa Ribero M, Jouvenet N, Dreux M, Nisole S. Interplay between SARS-CoV-2 and the type I interferon response. PLoS Pathog. 2020;16:e1008737. https://doi.org/10.1371/journal.ppat.1008737
7. Lamers MM, Haagmans BL. SARS-CoV-2 pathogenesis. Nat Rev Microbiol. 2022;20:270–84. https://doi.org/10.1038/s41579-022-00713-0
8. Guo K, Barrett BS, Morrison JH, Mickens KL, Vladar EK, Hasenkrug KJ, et al. Interferon resistance of emerging SARS-CoV-2 variants. Proc Natl Acad Sci U S A. 2022; 119:e2203760119. https://doi.org/10.1073/pnas.2203760119

9. Zhang Q, Bastard P, Liu Z, Le Pen J, Moncada-Velez M, Chen J, et al.; COVID-STORM Clinicians; COVID Clinicians; Imagine COVID Group; French COVID Cohort Study Group; CoV-Contact Cohort; Amsterdam UMC Covid-19 Biobank; COVID Human Genetic Effort; NIAID-USUHS/TAGC COVID Immunity Group. Inborn errors of type I IFN immunity in patients with life-threatening COVID-19. Science. 2020;370:eabd4570. https://doi.org/10.1126/science.abd4570
10. Banerjee A, Nasir JA, Budylowski P, Yip L, Aftanas P, Christie N, et al. Isolation, sequence, infectivity, and replication kinetics of severe acute respiratory syndrome coronavirus 2. Emerg Infect Dis. 2020;26:2054–63. https://doi.org/10.3201/eid2609.201495
11. Kotwa JD, Jamal AJ, Mbareche H, Yip L, Aftanas P, Barati S, et al. Surface and air contamination with severe acute respiratory syndrome coronavirus 2 from hospitalized coronavirus disease 2019 patients in Toronto, Canada, March–May 2020. J Infect Dis. 2022;225:768–76. https://doi.org/10.1093/infdis/jiab578
12. Elbe S, Buckland-Merrett G. Data, disease and diplomacy: GISAID's innovative contribution to global health. Glob Chall. 2017;1:33–46. https://doi.org/10.1002/gch2.1018
13. Kandel CE, Young M, Serbanescu MA, Powis JE, Bulir D, Callahan J, et al. Detection of severe acute respiratory coronavirus virus 2 (SARS-CoV-2) in outpatients: a multicenter comparison of self-collected saline gargle, oral swab, and combined oral-anterior nasal swab to a provider collected nasopharyngeal swab. Infect Control Hosp Epidemiol. 2021;42:1340–4. https://doi.org/10.1017/ice.2021.2
14. Carabelli AM, Peacock TP, Thorne LG, Harvey WT, Hughes J, Peacock SJ, et al.; COVID-19 Genomics UK Consortium. SARS-CoV-2 variant biology: immune escape, transmission and fitness. Nat Rev Microbiol. 2023;21:162–77. https://doi.org/10.1038/s41579-022-00841-7
15. Detsky AS, Bogoch II. COVID-19 in Canada: experience and response to waves 2 and 3. JAMA. 2021;326:1145–6. https://doi.org/10.1001/jama.2021.14797
16. Liu Y, Liu J, Plante KS, Plante JA, Xie X, Zhang X, et al. The N501Y spike substitution enhances SARS-CoV-2 infection and transmission. Nature. 2022;602:294–9. https://doi.org/10.1038/s41586-021-04245-0
17. Luan B, Wang H, Huynh T. Enhanced binding of the N501Y-mutated SARS-CoV-2 spike protein to the human ACE2 receptor: insights from molecular dynamics simulations. FEBS Lett. 2021;595:1454–61. https://doi.org/10.1002/1873-3468.14076
18. Laffeber C, de Koning K, Kanaar R, Lebbink JHG. Experimental evidence for enhanced receptor binding by rapidly spreading SARS-CoV-2 variants. J Mol Biol. 2021;433:167058. https://doi.org/10.1016/j.jmb.2021.167058
19. Plante JA, Mitchell BM, Plante KS, Debbink K, Weaver SC, Menachery VD. The variant gambit: COVID-19's next move. Cell Host Microbe. 2021;29:508–15. https://doi.org/10.1016/j.chom.2021.02.020
20. Tao K, Tzou PL, Nouhin J, Gupta RK, de Oliveira T, Kosakovsky Pond SL, et al. The biological and clinical significance of emerging SARS-CoV-2 variants. Nat Rev Genet. 2021;22:757–73. https://doi.org/10.1038/s41576-021-00408-x
21. Gu H, Chen Q, Yang G, He L, Fan H, Deng YQ, et al. Adaptation of SARS-CoV-2 in BALB/c mice for testing vaccine efficacy. Science. 2020;369:1603–7. https://doi.org/10.1126/science.abc4730
22. Tegally H, Wilkinson E, Giovanetti M, Iranzadeh A, Fonseca V, Giandhari J, et al. Detection of a SARS-CoV-2 variant of concern in South Africa. Nature. 2021;592:438–43. https://doi.org/10.1038/s41586-021-03402-9
23. Planas D, Bruel T, Grzelak L, Guivel-Benhassine F, Staropoli I, Porrot F, et al. Sensitivity of infectious SARS-CoV-2 B.1.1.7 and B.1.351 variants to neutralizing antibodies. Nat Med. 2021;27:917–24. https://doi.org/10.1038/s41591-021-01318-5
24. Wang P, Nair MS, Liu L, Iketani S, Luo Y, Guo Y, et al. Antibody resistance of SARS-CoV-2 variants B.1.351 and B.1.1.7. Nature. 2021;593:130–5. https://doi.org/10.1038/s41586-021-03398-2
25. Cele S, Gazy I, Jackson L, Hwa SH, Tegally H, Lustig G, et al.; Network for Genomic Surveillance in South Africa; COMMIT-KZN Team. Escape of SARS-CoV-2 501Y.V2 from neutralization by convalescent plasma. Nature. 2021;593:142–6. https://doi.org/10.1038/s41586-021-03471-w
26. Banerjee A, Lew J, Kroeker A, Baid K, Aftanas P, Nirmalarajah K, et al. Immunogenicity of convalescent and vaccinated sera against clinical isolates of ancestral SARS-CoV-2, Beta, Delta, and Omicron variants. Med. 2022;3:422–432.e3. https://doi.org/10.1016/j.medj.2022.04.002
27. Banerjee A, El-Sayes N, Budylowski P, Jacob RA, Richard D, Maan H, et al. Experimental and natural evidence of SARS-CoV-2-infection-induced activation of type I interferon responses. iScience. 2021;24:102477. https://doi.org/10.1016/j.isci.2021.102477
28. Lowery SA, Sariol A, Perlman S. Innate immune and inflammatory responses to SARS-CoV-2: implications for COVID-19. Cell Host Microbe. 2021;29:1052–62. https://doi.org/10.1016/j.chom.2021.05.004
29. Diamond MS, Kanneganti TD. Innate immunity: the first line of defense against SARS-CoV-2. Nat Immunol. 2022;23:165–76. https://doi.org/10.1038/s41590-021-01091-0
30. Chu H, Chan JF, Yuen TT, Shuai H, Yuan S, Wang Y, et al. Comparative tropism, replication kinetics, and cell damage profiling of SARS-CoV-2 and SARS-CoV with implications for clinical manifestations, transmissibility, and laboratory studies of COVID-19: an observational study. Lancet Microbe. 2020;1:e14–23. https://doi.org/10.1016/S2666-5247(20)30004-5
31. Mellott DM, Tseng CT, Drelich A, Fajtová P, Chenna BC, Kostomiris DH, et al. A clinical-stage cysteine protease inhibitor blocks SARS-CoV-2 infection of human and monkey cells. ACS Chem Biol. 2021;16:642–50. https://doi.org/10.1021/acschembio.0c00875
32. Mathema B, Chen L, Wang P, Cunningham MH, Mediavilla JR, Chow KF, et al. Genomic epidemiology and serology associated with a SARS-CoV-2 R.1 variant outbreak in New Jersey. MBio. 2022;13:e0214122. https://doi.org/10.1128/mbio.02141-22
33. Sholukh AM, Fiore-Gartland A, Ford ES, Miner MD, Hou YJ, Tse LV, et al. Evaluation of cell-based and surrogate SARS-CoV-2 neutralization assays. J Clin Microbiol. 2021;59:e0052721. https://doi.org/10.1128/JCM.00527-21
34. Lusvarghi S, Wang W, Herrup R, Neerukonda SN, Vassell R, Bentley L, et al. Key substitutions in the spike protein of SARS-CoV-2 variants can predict resistance to monoclonal antibodies, but other substitutions can modify the effects. J Virol. 2022;96:e0111021. https://doi.org/10.1128/JVI.01110-21

Address for correspondence: Karen Mossman, McMaster University, MDCL 5026, 1280 Main St W, Hamilton, ON L8S4K1, Canada; email: mossk@mcmaster.ca

Article DOI: https://doi.org/10.3201/eid2907.230198

Sensitivity to Neutralizing Antibodies and Resistance to Type I Interferons in SARS-CoV-2 R.1 Lineage Variants, Canada

Appendix

Supplementary Methods

Cell Lines

Vero E6 cells (ATCC CRL-1586) were cultured in Dulbecco's Modified Eagle's media (DMEM) supplemented with 10% fetal bovine serum, 1x L-glutamine, and 1% penicillin-streptomycin. Calu-3 cells (ATCC HTB-55) were cultured in Minimum Essential Medium (Alpha MEM) supplemented with 10% fetal bovine serum, 1x L-glutamine, and 1% penicillin-streptomycin.

SARS-CoV-2 viruses

The SARS-CoV-2 ancestral isolate, SB3 was isolated and purified as described previously (*1*). The B.1.351 (β) VoC, isolate was obtained from BEI Resources (Manassas, VA, United States). The R.1 lineage variant was isolated in this study from patient nasopharyngeal swabs collected in universal transport media. Briefly, samples were diluted in equal proportion with DMEM containing 16 µg/ml TPCK-trypsin (Cat. No. 4370285, Sigma-Aldrich) and inoculated on VeroE6 cells seeded the previous day in a 12-well plate. After 1h adsorption, the inoculum was replaced with DMEM containing 2% FBS and 6 µg/mL TPCK-trypsin. The cells were observed daily for CPE and cell culture supernatants collected once positive for CPE. A 140 µl aliquot was used for viral RNA extraction using the Qiagen viral RNA extraction kit (Cat. No. 52904). The detection of SARS-CoV-2 RNA was performed using a qRT-PCR as previously described (*2*). $TCID_{50}$ assay was used to quantify the virus stock titers in Vero E6 cell (*1*).

Experiments with SARS-CoV-2 were performed in a biosafety containment level 3 facility and all procedures were approved by the institutional biosafety committee at McMaster University.

Human donors

Informed consent was obtained for the collection of convalescent serum from 39 patients with laboratory confirmed SARS-CoV-2 infection. The data on sex and age were collected from all the participants. This study was approved by the institutional review board for Sunnybrook Research Institute (REB#2218) and Sinai Health System (REB# 02–0118-U and 05–0016-C).

Sequencing and bioinformatic analyses

Sequencing of SARS-CoV-2 genomes from RNA extracts and subsequent bioinformatics analysis followed the steps detailed in Kotwa *et al* (*3*). Briefly, after cDNA synthesis and generation of ARTIC3 amplicons, DNA sequencing libraries were constructed for paired-end 300 bp sequencing (Illumina MiSeq) with ~2000x fold coverage. Short-read sequence processing and genome assembly was done using the SIGNAL (SARS-CoV-2 Illumina GeNome Assembly Line) pipeline (https://github.com/jaleezyy/covid-19-signal) to generate genome consensus, determine mutations relative to the ancestral Wuhan genome (MN908947.3), and to predict PANGOLIN lineage (*4*). Quality of consensus genome and overall sequencing was assessed using NCoV-Tools (https://github.com/jts/ncov-tools).

Phylogenetic tree

Dataset consisted of study sequences (R.1 645, R.1 646 and SB3), Los Alamos National Laboratories (LANL) full-length variant reference alignment from GISAID Web site (*5*), and randomly sampled α, β and gamma VoC sequences. Multiple sequence alignment was executed using MAFFT (*6*,*7*). A maximum likelihood (ML) tree was constructed with RaxML (*8*) by executing 1000 rapid bootstrap inferences and a thorough ML search using General Time Reversible model of nucleotide substitution. The tree was visualized using FigTree v1.4.2 (*9*).

Detection of SARS-CoV-2–specific binding antibodies

The IgG antibodies targeting the RBD were determined using the BioLegend LEGEND MAX SARS-CoV-2 Spike RBD Human IgG ELISA kit (Cat. No. 447707, BioLegend). The IgG antibodies targeting the spike S1 region were determined using the LEGEND MAX SARS-CoV-2 Spike S1 Human IgG ELISA kit (Cat. No.447807, BioLegend). The ELISA was performed according to the manufacturer's instructions. Briefly, plates were washed four times with 300 µl

of 1x wash buffer. Next, human IgG standard were diluted 2-fold in assay buffer B. The standards ranged from 20 ng/ml to 0.313 ng/ml with 50 µl of standard per well. The serum samples were also diluted in assay buffer and 50 µl was added per well. The plates were sealed and incubated for 2 hours at room temperature with no shaking and washed four times with 300 µl of 1x wash buffer. Next, 100 µl of IgG detection antibody solution was added to each well. The plates were incubated at room temperature for 1 hour with no shaking and washed four times with 300 µl of 1x wash buffer. Next, 100 µl of Avidin-HRP solution was added to each well. The plates were incubated at room temperature for 1 hour with no shaking and washed five times with 300 µl of 1x wash buffer. Finally, 100 µl of substrate solution was added to each well and incubated for 10 minutes in the dark. The reaction was stopped by adding 100 µl of stop solution to each well. The absorbance was read at 450 nm within 10 minutes using the SpectraMax 190 microplate reader (Molecular Devices) at an optical density of 450 nm.

Molecular detection of SARS-CoV-2 RNA and $N_{501}Y$ mutation

Diagnostic nasopharyngeal or mid-turbinate swabs were collected from patients for SARS-CoV-2 testing and $N_{501}Y$ screening at Shared Hospital Laboratory (Toronto, Canada). RNA extraction and reverse transcription polymerase chain reactions (qRT-PCR) for SARS-CoV-2 detection were performed as previously described (*10*). In brief, RNA was extracted from 160 µl of sample using the MGISP-960 automated platform and the MGI Easy Magnetic Beads Virus DNA/RNA Extraction Kit (MGI Technologies, Shenzhen, China). qRT-PCR was performed using the CFX96 Touch Real-time PCR system (BioRad, Canada) with the envelope (E) gene, the 5′ untranslated region (5′ UTR), and the human RNase P internal control as targets. qRT-PCR for the $N_{501}Y$ screen was performed using the CFX96 Touch Real-time PCR (BioRad, Canada) and the Luna Universal Probe One-Step RT-qPCR Kit (New England Biolabs, Whitby, Ontario). Primer sequences used were: 501 Fwd – GAAGGTTTTAATTGTTACTTTC and 501 Rev – AAACAGTTGCTGGTGCATGT at 1.0 µM each. FAM-Y501 – CCAACCCACTTATGGTGTTG at 0.25 µM and HEX-N501 – CCAACCCACTAATGGTGTTG at 0.5 µM were the probe sequences used.

SARS-CoV-2 neutralization assay

Vero E6 cells were seeded at a density of $2.5x10^4$ cells per well in opaque 96-well flat-bottom plates in complete DMEM. Twenty-four hours later, patient serum was inactivated by incubating at 56°C for 30 minutes, then diluted 1:25 in low serum DMEM (supplemented with

2% FBS, 1x L-glutamine, and 1% penicillin-streptomycin). 2-fold serial dilution of the sample was performed in 96 well U-bottom plates. An equal volume of SARS-CoV-2 (15,000, 1,500 or 150 PFU/well) was then added to the diluted serum and the serum-virus mixture was incubated at 37°C for 1 hour. The Vero E6 culture media was then replaced with 100 µl of the serum-virus mixture and incubated at 37°C for 5 days. The plates were read by removing 50ul of culture supernatant and adding 50 µl of CellTiter-Glo 2.0 Reagent (Cat. No. G9243, Promega, Madison, WI, United States) to each well. The plates were then shaken at 282cpm at 3mm diameter for 2 minutes, incubated for 5 minutes at room temperature, then luminescence was read using a BioTek Synergy H1 microplate reader with a gain of 135 and integration time of 1 second.

Interferon treatment and quantitative PCR

Calu-3 cells were seeded at a density of $0.2x10^6$ cells/well in 12-well plates and infected with SARS-CoV-2 2 days post-seeding. The cells were either mock-infected or SARS-CoV-2 infected (50,000 PFU/well). Soon after the 1 h post-adsorption time, wells were washed twice with 1xPBS and treated with recombinant IFN-α (Cat. No. I4276, Sigma-Aldrich) or IFNβ (Cat. No. 300–02BC, PeproTech). RNA extraction was performed using RNeasy Mini Kit (Cat No. 74106, Qiagen) according to the manufacturer's protocol after 72 h post-infection. Five hundred nanograms of purified RNA were reverse transcribed using iScript gDNA Clear cDNA Synthesis Kit (Cat. No. 1725035, Bio-Rad). To quantify SARS-CoV-2 RNA qRT-PCR was performed using SsoFast EvaGreen supermix (Cat. No. 1725211, Bio-Rad) using the following primers: upE Fwd – ATTGTTGATGAGCCTGAAG and upE Rev – TTCGTACTCATCAGCTTG. To quantify ISGs, qRT-PCR reactions were performed with Taqman Universal PCR master mix using pre-designed Taqman gene expression assays (Thermo Fisher Scientific, Massachusetts, United States) for *GAPDH* (Cat. No. 4331182), *IFIT1* (Cat. No. 4331182) and *IRF7* (Cat. No. 4331182) according to manufacturer's protocol.

Viability assay

Calu-3 cells seeded in 12-well plates were either mock-infected or SARS-CoV-2 infected (1 hour exposure, 50,000 PFU/well), washed twice with sterile 1x PBS, and treated with recombinant IFN-α (Cat. No. I4276, Sigma-Aldrich) or IFNβ (Cat. No. 300–02BC, PeproTech). Two different concentrations of interferon were used for the assay (1ng/ml and 10 ng/ml). Cell viability was assessed by adding an equal volume of CellTiter-Glo 2.0 Reagent (Promega, Madison, WI, United States), mixed and lysates transferred to opaque 96-well flat-bottom plates

with six replicates per well. The plates were then shaken at 282cpm at 3mm diameter for 2 minutes and luminescence was read using a BioTek Synergy H1 microplate reader with a gain of 135 and integration time of 1 second.

Statistical analysis

All statistics were performed using Graph Pad Prism (Graph Pad Software, Inc., La Jolla, CA). An unpaired t test was used for Figure 2A, B. The correlations for Figure 2C, D and Appendix Figure 2, panels D–F were analyzed using Spearman r. One-way AVOVA with Tukey's multiple comparisons test was used to make comparisons in Figure 2E-G and Figure 3A-F. Two-way ANOVA with Tukey's multiple comparisons test was used for multiple comparisons in Figure 4. The ID_{50} values were calculated using a nonlinear regression model for Appendix Figure 1A-I and Appendix Figure 2A-C. The following p values were considered significant: *$p < 0.05$, **$p < 0.01$, and ***$p < 0.001$, ****$p < 0.0001$.

References

1. Banerjee A, Nasir JA, Budylowski P, Yip L, Aftanas P, Christie N, et al. Isolation, sequence, infectivity, and replication kinetics of severe acute respiratory syndrome coronavirus 2. Emerg Infect Dis. 2020;26:2054–63. PubMed https://doi.org/10.3201/eid2609.201495

2. Banerjee A, El-Sayes N, Budylowski P, Jacob RA, Richard D, Maan H, et al. Experimental and natural evidence of SARS-CoV-2-infection-induced activation of type I interferon responses. iScience. 2021;24:102477. PubMed https://doi.org/10.1016/j.isci.2021.102477

3. Kotwa JD, Jamal AJ, Mbareche H, Yip L, Aftanas P, Barati S, et al. Surface and air contamination with severe acute respiratory syndrome coronavirus 2 from hospitalized coronavirus disease 2019 patients in Toronto, Canada, March–May 2020. J Infect Dis. 2022;225:768–76. PubMed https://doi.org/10.1093/infdis/jiab578

4. Nasir JA, Kozak RA, Aftanas P, Raphenya AR, Smith KM, Maguire F, et al. A comparison of whole genome sequencing of SARS-CoV-2 using amplicon-based sequencing, random hexamers, and bait capture. Viruses. 2020;12:895. PubMed https://doi.org/10.3390/v12080895

5. Elbe S, Buckland-Merrett G. Data, disease and diplomacy: GISAID's innovative contribution to global health. Glob Chall. 2017;1:33–46. PubMed https://doi.org/10.1002/gch2.1018

6. Katoh K, Standley DM. MAFFT multiple sequence alignment software version 7: improvements in performance and usability. Mol Biol Evol. 2013;30:772–80. PubMed https://doi.org/10.1093/molbev/mst010

7. Katoh K, Misawa K, Kuma K, Miyata T. MAFFT: a novel method for rapid multiple sequence alignment based on fast Fourier transform. Nucleic Acids Res. 2002;30:3059–66. PubMed https://doi.org/10.1093/nar/gkf436

8. Stamatakis A. RAxML version 8: a tool for phylogenetic analysis and post-analysis of large phylogenies. Bioinformatics. 2014;30:1312–3. PubMed https://doi.org/10.1093/bioinformatics/btu033

9. Molecular evolution, phylogenetics and epidemiology [cited 2023 Feb 1]. http://tree.bio.ed.ac.uk

10. Kandel CE, Young M, Serbanescu MA, Powis JE, Bulir D, Callahan J, et al. Detection of severe acute respiratory coronavirus virus 2 (SARS-CoV-2) in outpatients: A multicenter comparison of self-collected saline gargle, oral swab, and combined oral-anterior nasal swab to a provider collected nasopharyngeal swab. Infect Control Hosp Epidemiol. 2021;42:1340–4. PubMed https://doi.org/10.1017/ice.2021.2

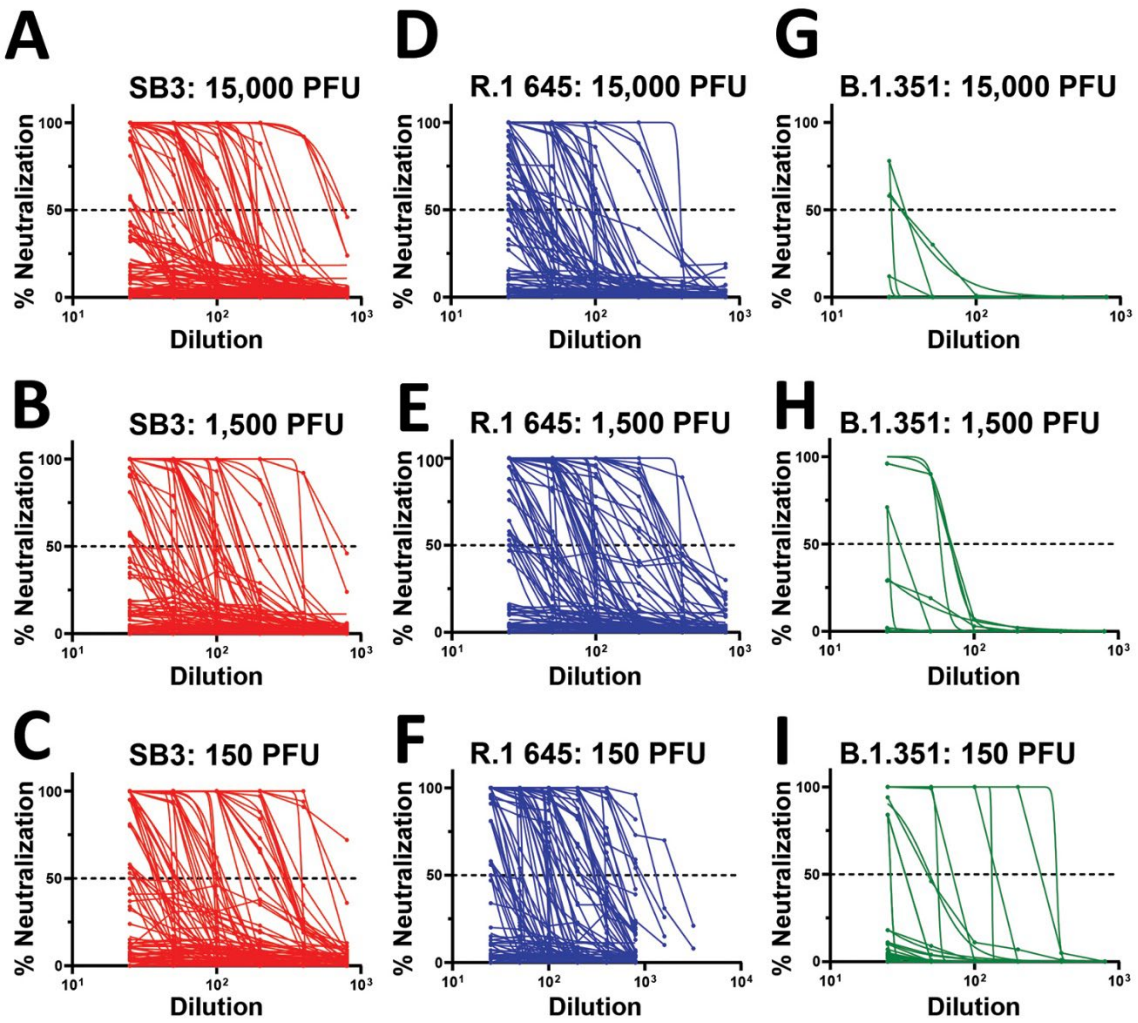

Appendix Figure 1. Regression line depicting the neutralization activity of the 39 convalescent serum samples tested on the three SARS-CoV-2 isolates. A PFU/well of 15,000, 1,500 and 150 were used for each of the SARS-CoV-2 isolates. (A-C) Neutralization profile of SB3. (D-F) Neutralization profile of R.1 645. (G-I) Neutralization profile of B.1.351 (Beta) VoC.

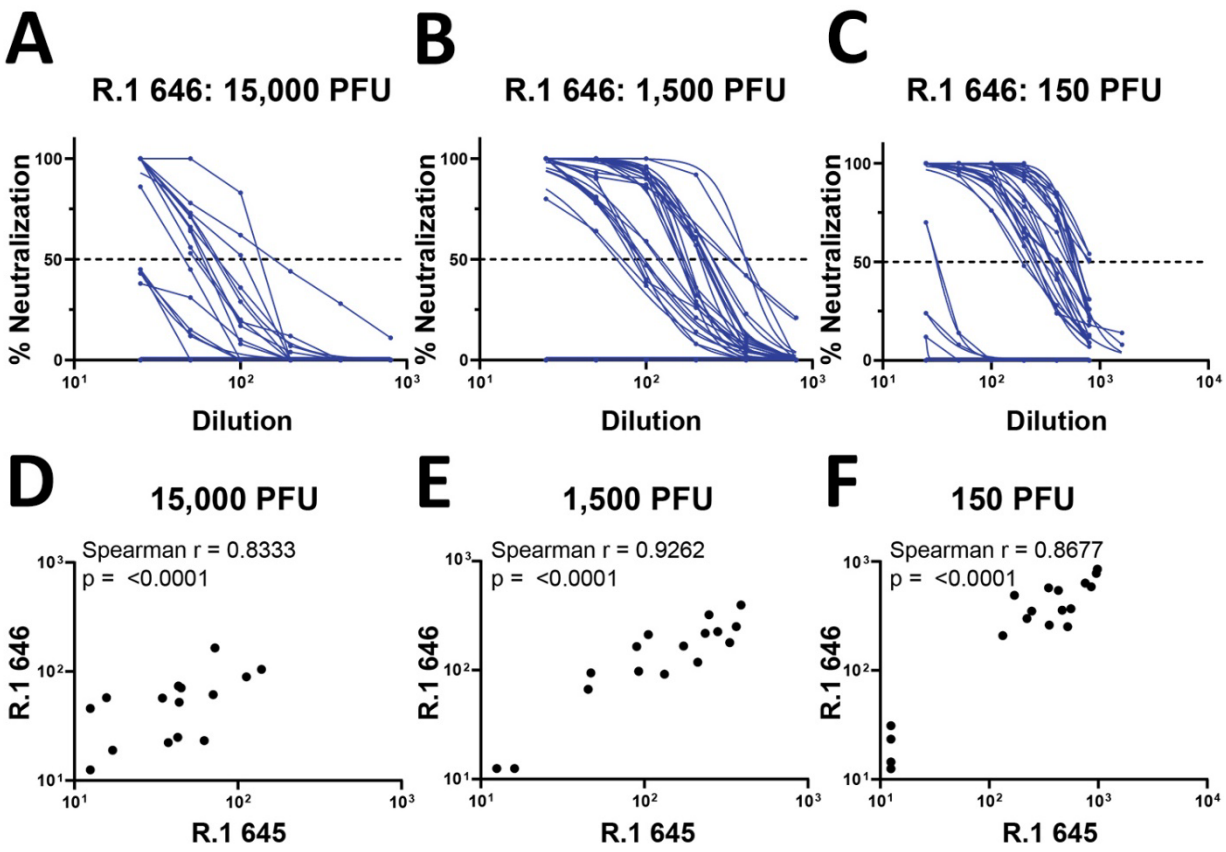

Appendix Figure 2. (A-C) Regression line depicting the neutralization activity of a subset of the convalescent serum samples (n = 19) to R.1 646. A PFU/well of 15,000, 1,500 and 150 were used. (D-F) ID_{50} titer correlation between R.1 645 and R.1 646 for 15,000, 1,500 and 150 PFU/well.

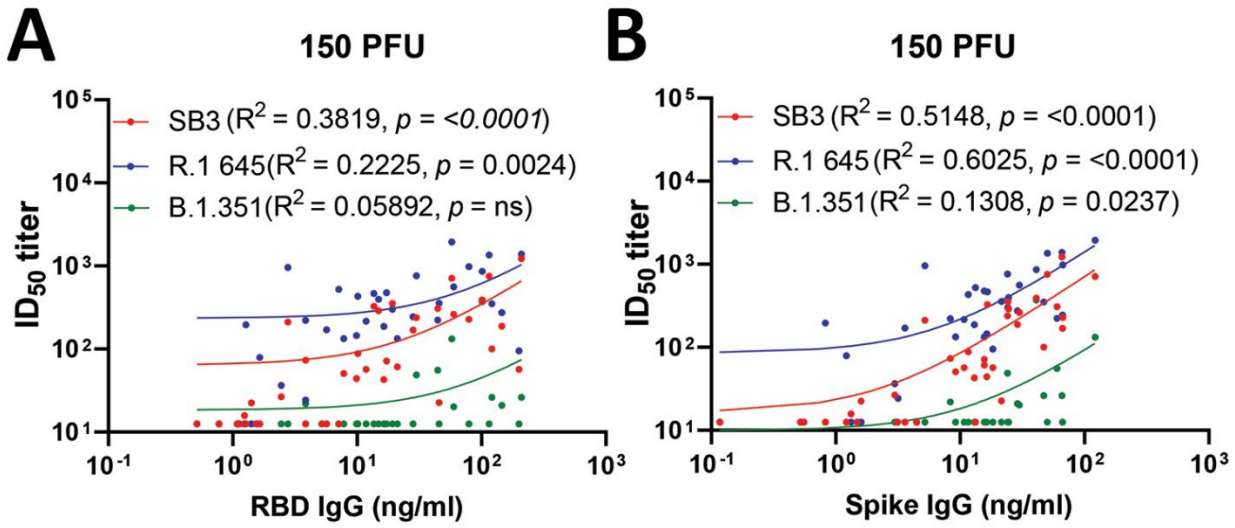

Appendix Figure 3. (A) Predicting neutralization of SB3, R,1 645 and B.1.351 (Beta) VoC (150 PFU/well) using RBD binding IgG antibodies. (B) Predicting neutralization of SB3, R,1 645 and B.1.351 (Beta) VoC (150 PFU/well) using spike (S1) binding IgG antibodies. The R-squared values were calculated using a simple linear regression model. (ns-not significant)

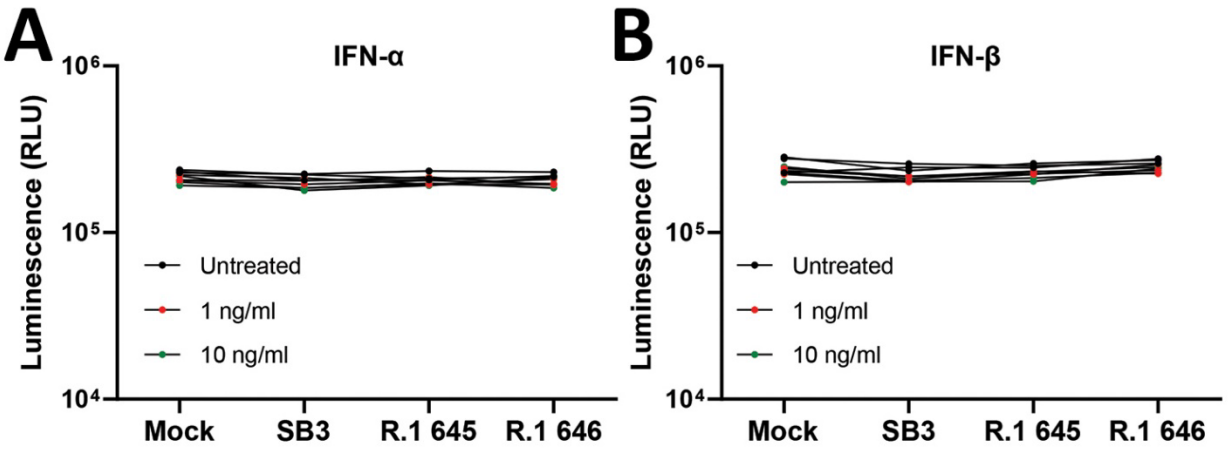

Appendix Figure 4. (A, B) Calu-3 cells were either mock-infected or infected with SARS-CoV-2 (50,000 PFU/well) for 1 h followed by treatment with recombinant IFNα (1 or 10 ng/mL) or IFNβ (1 or 10 ng/mL). Seventy-two hours later, viability was assessed using CellTiter-Glo 2.0 reagent and luminescence measured using a BioTek Synergy H1 microplate reader.

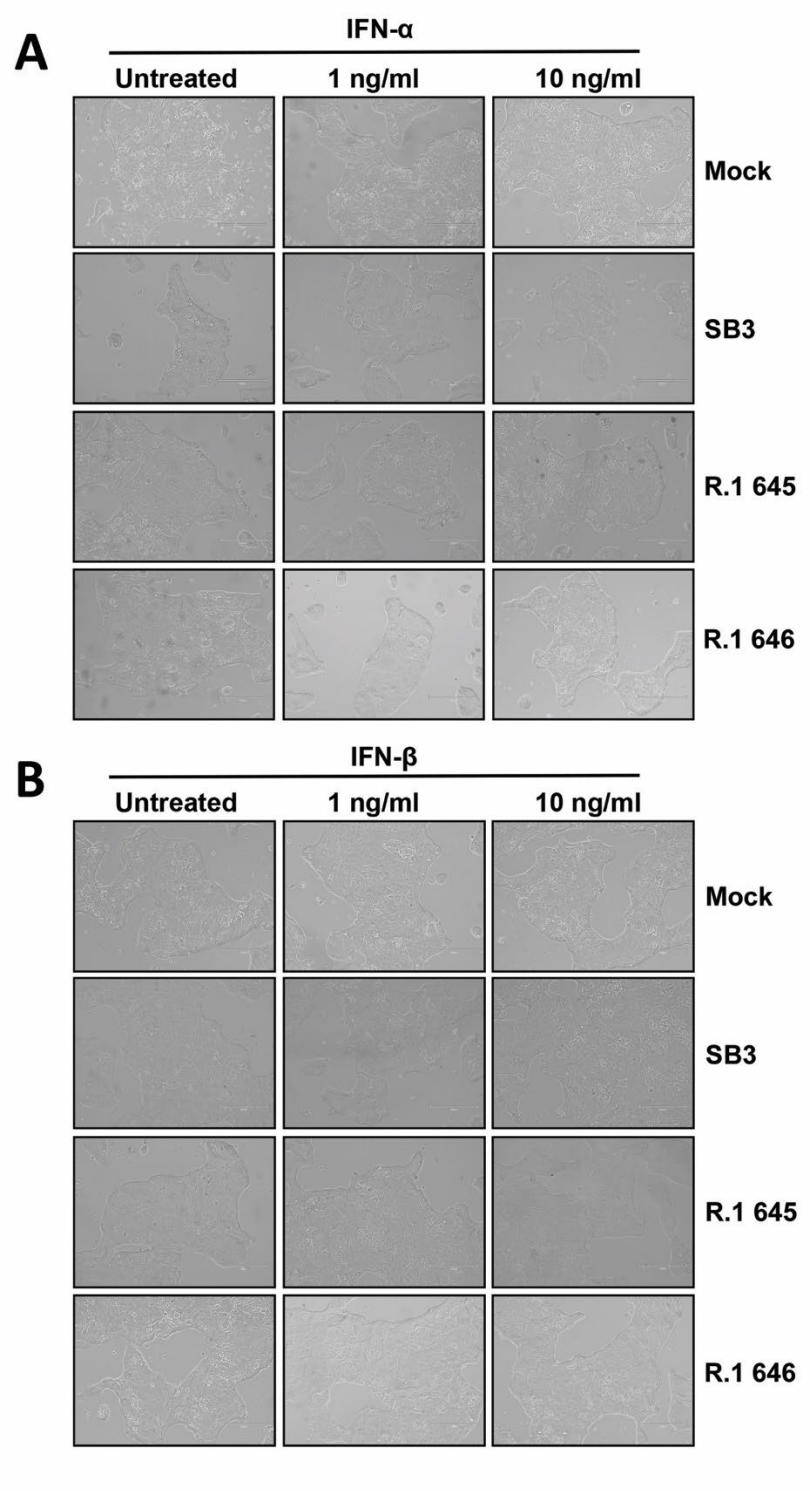

Appendix Figure 5. (A, B) Calu-3 cells were either mock-infected or infected with SARS-CoV-2 (50,000 PFU/well) for 1 h followed by treatment with recombinant IFNα (1 or 10 ng/mL) or IFNβ (1 or 10 ng/mL). Seventy-two hours later, cells were imaged using a EVOS M5000 microscope. Images shown are representative cells from three replicates for each condition. The scale bar is 300 μm.